Sustainable Chemistry

Efficient Photocatalytic Oxidation of Aromatic Alcohols over Thiophene-based Covalent Triazine Frameworks with A Narrow Band Gap

Longfei Liao,[a] Daniel Ditz,[a] Feng Zeng,[a] Marcelo Alves Favaro,[a] Andree Iemhoff,[a] Kavita Gupta,[a] Heinrich Hartmann,[b] Conrad Szczuka,[c, d] Peter Jakes,[c] Peter J. C. Hausoul,[a] Jens Artz,*[a] and Regina Palkovits*[a]

Photocatalytic selective oxidation of aromatic alcohols by covalent organic frameworks (COFs) is a sustainable strategy to replace present metal-based heterogeneous catalytic oxidation systems. Covalent triazine-based frameworks (CTFs), a subgroup of COFs, possess promising properties as efficient catalysts for photocatalytic oxidation. Sulfur-containing metal-free CTFs exhibit a good performance in photocatalysis due to their narrowed band gap, and the fast generated photo-electrons/holes separation and transfer. Here, we report the synthesis of thiophene-based CTFs under mild conditions for photocatalytic oxidation of aromatic alcohols to the corresponding benzaldehydes using pure oxygen as the oxidant. Full conversion and a selectivity as high as 90% to benzaldehyde were obtained paving the way for a potential application of these metal-free photocatalysts in fine chemicals synthesis.

1. Introduction

The catalytic selective oxidation of aromatic alcohols to the corresponding aldehydes or ketones is a critical reaction for fine chemicals and intermediates in the chemical industry.[1–4] Traditionally, transition metals oxidants such as CrO^{3-} or MnO^{4-} were employed to oxidize aromatic alcohols, producing a large amount of by-products.[2,5–7] Photocatalytic oxidation using metal-free photocatalysts presents a simple and environmentally benign alternative overcoming these limitations.[8–18] In recent years, the development of metal-free photocatalysts has attracted great attention among researchers.[9,19–23] Among them are many classes of porous organic polymers (POPs), including conjugated microporous polymers (CMPs),[24–26] covalent organic frameworks (COFs),[11–14] and porous aromatic frameworks (PAFs) and so forth. Covalent triazine frameworks (CTFs) present a promising material class for photocatalytic applications. They hold a triazine unit (aromatic C=N linkage) as a structural element and possess stable covalent bonds.[24–26,30] Different approaches for the synthesis of CTFs have been reported including high-temperature ionothermal trimerization, reported by Thomas *et al.* However, the method causes partial carbonization and results in black powders not suitable for photocatalysis.[31–33] Besides, CTFs can also be synthesized using trifluoromethanesulfonic acid as a catalyst at room temperature or by microwave heating both avoiding carbonization.[34–36] Although these methods allow overcoming the major challenge of high-temperature synthesis, the routes are not ideal both considering safety and applicability for acid-sensitive building blocks.[17,20–22]

Recently, a novel mild synthesis approach for CTFs via polymerization of amidine and aldehyde monomers has been reported and the resulting CTFs appear promising for photocatalytic reactions owing to a good light absorbance and variable CTF structure available by careful monomer selection.[26,29,30] According to this method, CTFs can be synthesized under gentle reaction conditions without the need for strong acids. The resulting materials provide unique characteristics, such as layered structures, tunable functions, and high surface areas.[37] More importantly, these CTFs cannot only be applied for energy storage but also present promising materials in photocatalysis. More specifically, the strong aromatic bonds of the triazine unit provide some special property for CTFs, which offer great potential for many catalytic applications and the attractive heteroatom effect (HAE).[21,22]

[a] L. Liao, D. Ditz, Dr. F. Zeng, Dr. M. Alves Favaro, A. Iemhoff, Dr. K. Gupta, Dr. P. J. C. Hausoul, Dr. J. Artz, Prof. R. Palkovits
Institut für Technische und Makromolekulare Chemie(ITMC), RWTH Aachen University Aachen 52074 (Germany)
E-mail: artz@itmc.rwth-aachen.de
palkovits@itmc.rwth-aachen.de
[b] Dr. H. Hartmann
Zentralinstitut für Engineering, Elektronik und Analytik ZEA-3: Analytik Forschungszentrum Jülich GmbH 52425 Jülich (Germany)
[c] C. Szczuka, Dr. P. Jakes
Forschungszentrum Jülich, Institut für Energie- und Klimaforschung Grundlagen der Elektrochemie (IEK-9) 52425 Jülich (Germany)
[d] C. Szczuka
Institute of Physical Chemistry, RWTH Aachen University, 52074 Aachen (Germany)

Supporting information for this article is available on the WWW under https://doi.org/10.1002/slct.202004115

© 2020 The Authors. ChemistrySelect published by Wiley-VCH GmbH. This is an open access article under the terms of the Creative Commons Attribution Non-Commercial License, which permits use, distribution and reproduction in any medium, provided the original work is properly cited and is not used for commercial purposes.

Thiophene, a strong electron-donating chromophore, has been widely applied as key structural element for opto-related electronic polymers, serving as the chromophoric center to collect photons.[44–46] The incorporation of thiophene groups into photocatalytic materials adapts the electronic structure, tuning LUMO and HOMO positions, and narrows the band gap.[47] Enhanced photocatalytic performance of materials modified with thiophene groups compared to other photocatalysts has been demonstrated recently.

Herein, we report a new method for the synthesis of sulfur-containing CTFs via the amidine-aldehyde method and the application of them as metal-free catalysts for the photooxidation of aromatic alcohols. Aldehyde- and amidine-based monomers were assembled to different covalent triazine frameworks (Scheme 1a). In ancient times, the scaffolds of the wooden house were connected by robust Kongming lock (joint),[48] combining multiple mortises with tenons (Scheme 1b), which parallels the amidine-aldehyde method to synthesize a range of triazine-linked stable CTFs. CTFs composed of thiophene building blocks with sulfur promotion potentially possess a narrower band gap and high thermal stability, compared to phenyl-based CTFs. The obtained CTF-PhTh enable high catalytic activity in the photocatalytic oxidation of benzaldehydes with close to 100% selectivity at 44.9% conversion, and a TOF of 0.449 mmol g^{-1}_{cat} h^{-1}, which is comparable to the state of the art metal-based catalysts, and among the most efficient metal-free systems.

2. Results and Discussion

To confirm the formation of the triazine unit, Fourier-transformed infrared (FT-IR) was used to analyze the synthesized CTFs materials. Characteristic vibrations of triazine units at 1505 cm^{-1}, 1342 cm^{-1}, and 802 cm^{-1} were observed for all CTFs, consistent with the signal positions of the CTF model compound (pink) in Figure 1a. Besides, the successful formation of the triazine units was further confirmed by solid-state ^{13}C cross-polarization magic-angle-spinning (CP-MAS) NMR analysis, where the chemical shifts at 138.1 ppm and 127.9 ppm can be assigned to phenyl carbons and the chemical shift at 169.2 ppm was attributed to the carbon signals of the triazine rings. The presence of sp^2 carbons is confirmed by the chemical shifts of thiophene rings in CTF-Th and CTF-PhTh located at 144.8 ppm and 137.7 ppm (Figure 1b).[49] The powder X-ray diffraction (PXRD) analysis indicated that despite the absence of long-range order in all CTFs, two broad reflexes at 6.6° and 20.2° occurred (Figure 1c), suggesting layered CTF structures.[37] In addition, Figure 1d illustrates that the CTFs possess a relatively high thermal stability of up to 600 °C, however, there is an obvious loss of mass from 600 °C to 700 °C. Elemental

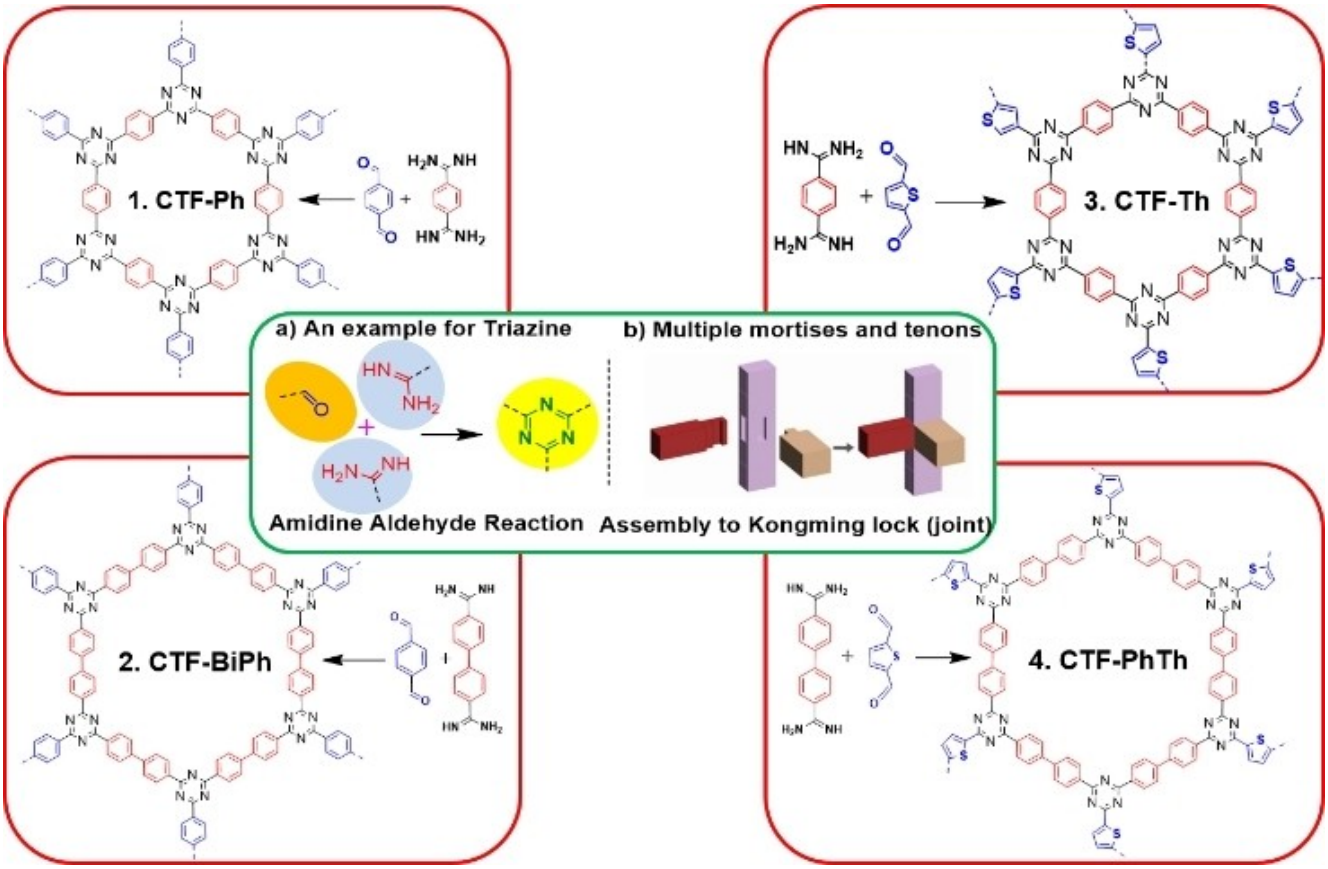

Scheme 1. Illustrated formation of thiophene-based CTFs (CTF-Th, CTF-PhTh) and phenyl-based CTFs (CTF-Ph, CTF-BiPh). (a) Amidine-aldehyde formation of triazine. (b) Ancient synthetic scaffolds combining multiple mortises and tenons. Previously reported CTF-HUST-1 named CTF-Ph here.[37]

© 2020 The Authors. ChemistrySelect published by Wiley-VCH GmbH

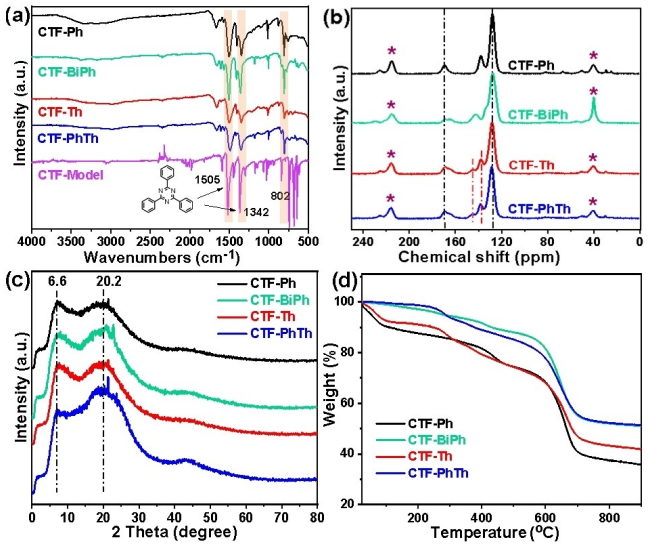

Figure 1. (a) FT-IR spectra, (b) ^{13}C CP-MAS NMR spectra (* represents spinning sideband), (c) PXRD spectra, and (d) TGA curves of the different CTFs.

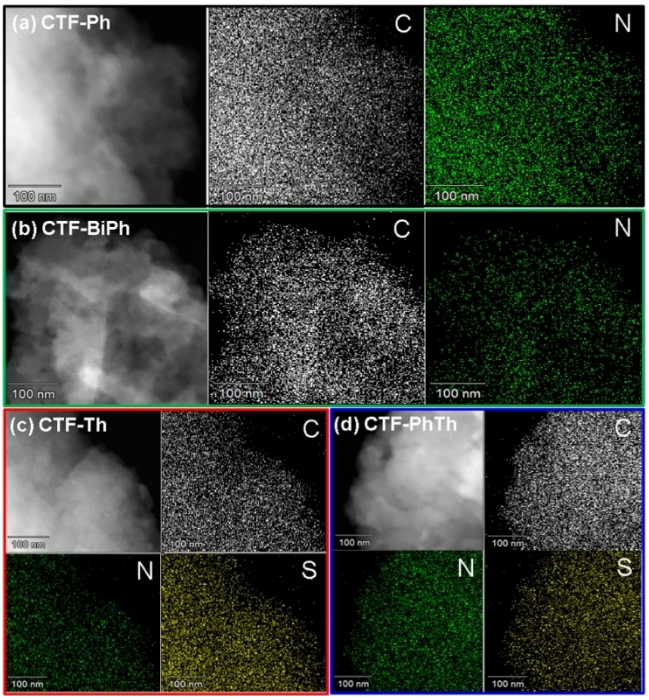

Figure 3. Typical STEM-EDS mapping images of CTFs and their corresponding elemental mappings of C, N, and S elements.

analysis was employed to analyze the elemental composition of the materials emphasizing a content of carbon and nitrogen close to the ideal structures (Table S1).

The CTFs morphologies were characterized by scanning electron microscopy (SEM) summarized in Figure 2, confirming a certain layered structure in the case of CTF-Th and bulk particles in CTF-Ph. Interestingly, a flower-like shape and cotton-liked structure were obtained for CTF-BiPh and CTF-PhTh, respectively. CTFs analyses by scanning transmission electron microscopy (STEM) with energy dispersive X-ray spectroscopy (EDS) indicates a uniform distribution of carbon, nitrogen, and sulfur in the CTFs (in Figures 3).

The surface of CTFs was analyzed using X-ray photoelectron spectroscopy (XPS) (in Figure 4a), O1s, N1s, and C1s peaks occur at 531.7 eV, 398.5 eV, and 284.0 eV, respectively. The peaks (227.9 eV and 164.0 eV) related to S 2 s and S 2p emphasize a thiophene-type chemical environment in CTF-Th and CTF-PhTh. The observed elemental compositional was in agreement with the observation made in the elemental analysis

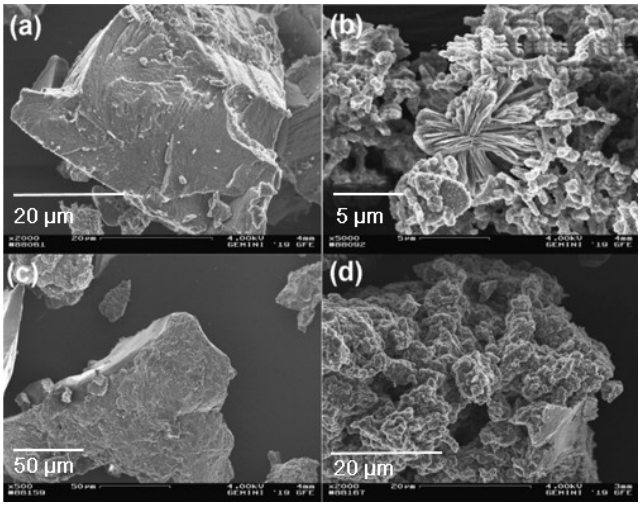

Figure 2. SEM images of CTF-Ph (a), CTF-BiPh (b), CTF-Th (c), and CTF-PhTh (d).

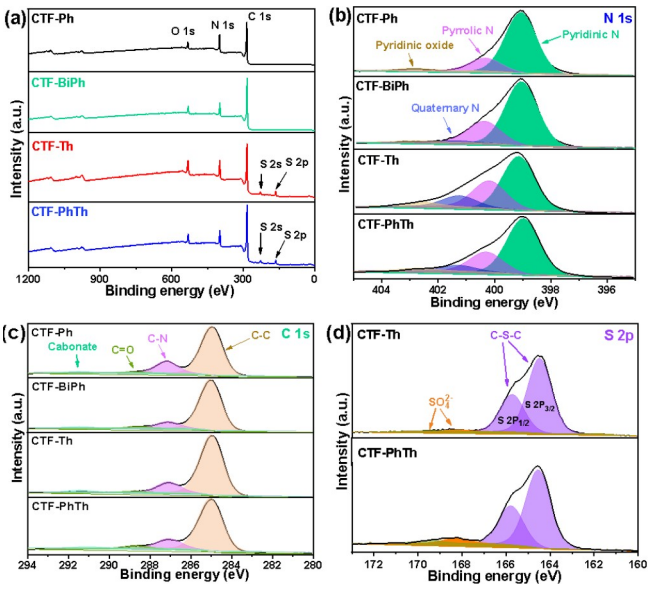

Figure 4. X-ray photoelectron spectroscopy survey (a), N 1s spectra (b), C 1s spectra (c) of all CTFs, and S 2p spectra of CTF-Th and CTF-PhTh (d).

© 2020 The Authors. ChemistrySelect published by Wiley-VCH GmbH

(Table S1). The high-resolution N 1s spectrum indicated three types of nitrogen in the CTFs with binding energies of 399.1 eV, 400.3 eV, and 402.7 eV, according to pyridinic nitrogen species in triazine units (C–N=C), pyrrolic nitrogen (C–N–C), and pyridine N–O nitrogen, respectively.[50] In addition, a weak signal at 401.3 eV occurred, potentially due to amide groups partly hydrolyzed to quaternary ammonium salts. Quaternary nitrogen and pyrrolic nitrogen originated from the 1,3,5-dihydrotriazine ring, generated by condensation of amidine and aldehyde monomers during synthesis. In the high-resolution C 1s spectrum, shown in Figure 4c, a main peak at 284.9 eV for carbon atoms (C–C) in phenyl and thiophene rings can be observed, two weak ones at 286.9 eV and 288.5 eV can be attributed to C–N in the triazine ring and C=O in imide groups.[49] Besides, the presence of sulfur in thiophene-based CTFs was also confirmed. In the high-resolution S 2p spectrum, two main energy peaks assigned to the thiophene units (C–S–C) at 164.4 eV and 165.7 eV appear, and an additional doublet with an S $2p_{3/2}$ and S $2p_{1/2}$ binding energy of 168.2 eV and 169.4 eV can be observed corresponding to sulfate group.[49]

UV-Visible diffuse reflectance spectroscopy (UV-Vis DRS) was carried to study the optical characteristics of all CTFs. Thiophene-based CTFs possess a maximum absorbance wavelength of approximately 550 nm, and therewith wider compared to phenyl-based CTFs with 400 nm/450 nm. However, the phenyl-based CTFs, CTF-Ph and CTF-BiPh show a significantly stronger absorbance compared to CTF–Th and CTF-PhTh. The UV-Vis spectra of CTFs can be used to calculate the related band gaps. Figure 5b illustrates that CTF-Th holds the narrowest band gap (1.78 eV) while CTF-BiPh holds the widest band gap of 2.84 eV. CTF-Ph and CTF-PhTh possess band gaps of 2.34 eV and 1.84 eV, respectively. Interestingly, thiophene-based CTFs provide a narrower band gap, which means electrons can be easily excited to pass through the band gap to reach the conduction band (CB) facilitating the photo-reaction. On the other hand, due to the larger ionic radius of sulfur, replacing nitrogen sites by sulfur sites clearly influences the electronic environment resulting in a narrower band gap in thiophene-based CTFs.[51] Photos of the CTFs materials (in Figure 5a) show that the colors are related to the absorption properties, with red color for thiophene-based CTFs, while phenyl-based CTFs are yellow powders.

The valence band maximum (VBM) and relative band positions for CTFs were evaluated by XPS measurements scanning a low binding energy range of 5 eV to −1 eV. Figure 5c illustrates that the binding energy of the valence electrons shifts comparing the different CTFs. CTF-BiPh possesses the largest valence band offset and the most negative valence band edge. According to typical XPS analysis, the binding energy for an electron can be used to determine how much energy the electron needs to occupy the whole Fermi level. Therefore, the valence band positions of CTFs can be evaluated as +1.58 eV, +1.37 eV, +0.94 eV, and +1.15 eV (*vs* NHE at pH = 0), for CTF-Ph, CTF-BiPh, CTF-Th, and CTF-PhTh, respectively. Considering the band gap calculated from UV-Vis spectra and the corresponding XPS valence band position, the conduction band positions of CTF-Ph, CTF-BiPh, CTF-Th, and CTF-PhTh could be estimated as −0.76 eV, −1.47 eV, −0.84 eV, and −0.69 eV (vs NHE at pH = 0), respectively. The conduction and valence band positions of CTFs are shown in Figure 5d and Table S2 in the electronic supplementary information. It is worth noting that phenyl-based CTFs possess relatively high conduction band potentials, thus supplying photo-oxidation with a greater driving force, while the band gaps of thiophene-based CTFs are much narrower, leading to lower energy for the electrons required for reaching the conduction band.[52]

Electrochemical experiments are effective to further evaluate the separation and transport of photo-generated carriers. As shown in Figure 6a, CTF-PhTh and CTF-BiPh exhibit the highest photocurrent densities, which are almost 2.3 and 2.7 folds of CTF-Ph, respectively, indicating their photo-generated carriers have higher separation and transfer efficiency of the photo-induced carriers. Moreover, all CTFs have good photoelectric stability, despite the seven periodic cycles of light on/

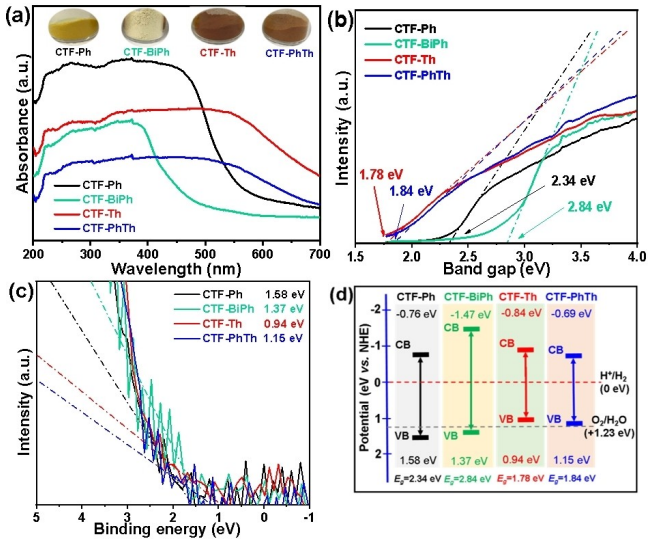

Figure 5. (a) UV-Vis absorption spectra of CTFs, (b) band gap spectra of CTFs, (c) valence band XPS spectra of CTFs, (d) estimated band structure diagrams of CTFs (CB: conduction band, VB: valence band). (NHE: Normal hydrogen electrode)

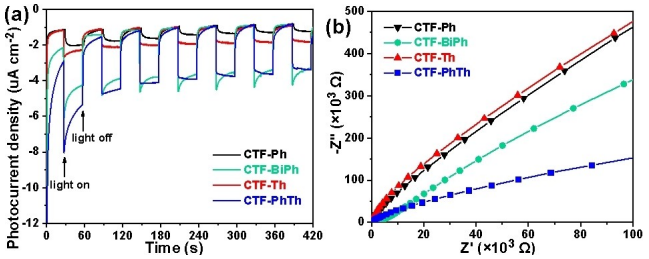

Figure 6. Photoelectrochemical properties of CTF-Ph, CTF-BiPh, CTF-Th, and CTF-PhTh. (a) Periodic on/off photocurrent response in 0.2 M Na_2SO_4 electrolyte with a FTO electrode under UV light irradiation (λ = 365 nm, 0.001231 W cm^{-2}) at −0.2 V vs. Ag/AgCl electrode; (b) Electrochemical impedance spectroscopy Nyquist plots in the dark.

© 2020 The Authors. ChemistrySelect published by Wiley-VCH GmbH

off treatment, the photocurrent density remains reversibly and reproducibly.

The electrical impedance spectroscopy (EIS) analysis in the dark (Figure 6b) shows that CTF-PhTh has the smallest Nyquist plot radius, followed by CTF-BiPh, while larger Nyquist plots radii were observed in CTF-Ph and CTF-Th, indicating that CTF-PhTh and CTF-BiPh have better charge conductivity, which is consistent with the tendency of the photocurrent response.

Electron paramagnetic resonance (EPR) can be used to observe radicals in CTFs. The presence of sulfur in the CTF materials has a significant impact on the electrical properties, which were determined by room-temperature EPR measurements with CTF-Ph and CTF-BiPh as references. The EPR intensities were greatly enhanced after incorporating sulfur, and the intensities followed the order CTF-Th > CTF-PhTh > CTF-Ph > CTF-BiPh (in Figure 7). The enhanced EPR intensities of the CTF-Th and CTF-PhTh samples demonstrated that the modification with sulfur atoms may effectively accelerate the electron mobility in the π-conjugated system of CTFs.[53]

In summary, we could successfully apply a mild synthesis protocol in the synthesis of conventional and sulfur functionalized CTFs. The thiophene-based CTFs possess a narrower band gap and provide more free radicals than phenyl-based CTFs, owing to the special structure containing sulfur atoms. However, phenyl-based CTFs show stronger light absorption. Despite the low surface area and absence of long-range order, the derived CTFs possess high thermal stability.

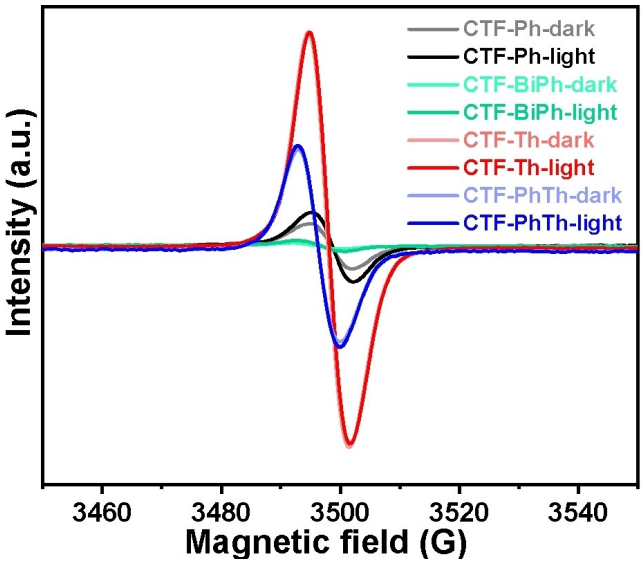

Figure 7. EPR spectra of CTFs obtained under UV light irradiation and in the dark.

2.1. Photocatalytic activity testing

To evaluate the photocatalytic characteristics of the different CTFs, the behavior in photo-oxidation of benzyl alcohol was investigated in Figure 8. All of the CTFs exhibit good catalytic performance reaching a benzaldehyde selectivity of 100% within 1 hour reaction time. Among all CTFs, CTF-Ph provides the lowest conversion with only 80% even after 10 hours reaction. In contrast, CTF-BiPh allows 100% conversion within 3 hours first selectively forming benzaldehyde which was quickly converted to benzoic acid. Although the thiophene-based CTFs required slightly longer reaction times to achieve a full conversion of benzyl alcohol to benzaldehyde, the subsequent further oxidation proceeded delayed allowing a selective benzaldehyde formation after 1 to 2 hours reaction time.

Light intensity also presents an important parameter influencing the reaction. Indeed, for a reaction time of 1 hour, the conversion of benzyl alcohol over CTF-PhTh rises with increasing light intensity (in Figure 9). This trend reveals that

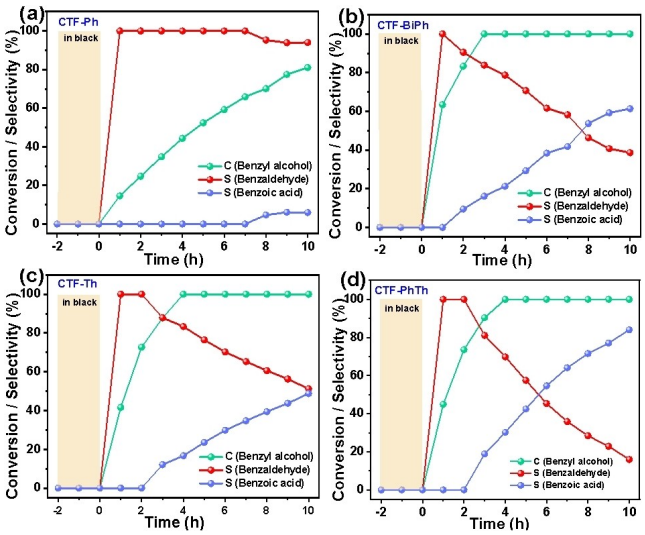

Figure 8. Oxidation of benzyl alcohol over CTFs dependent on reaction times. Reaction conditions: benzyl alcohol (5 μmol), acetonitrile (5.0 mL), photocatalyst (5.0 mg), UV light (λ = 365 nm, 0.1 W cm^{-2}), RT, O_2 balloon.

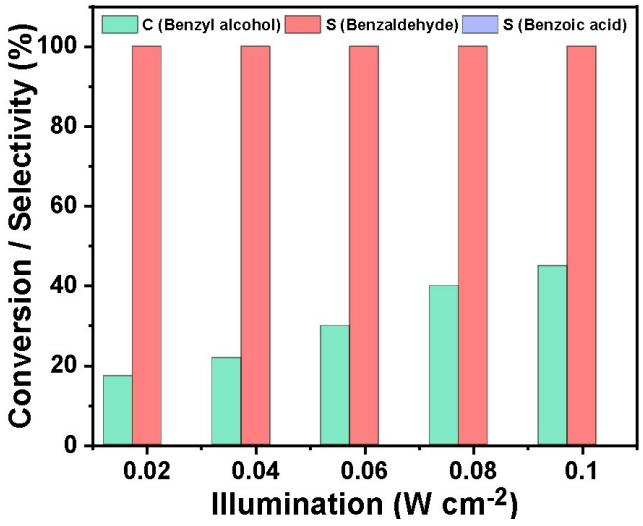

Figure 9. Oxidation conversion of benzyl alcohol over CTF-PhTh on various UV light intensity. Reaction conditions: benzyl alcohol (5 μmol), acetonitrile (5.0 mL), photocatalyst (5.0 mg), UV light (λ = 365 nm, 0.1 W cm^{-2}), 1 h, RT, O_2 balloon.

© 2020 The Authors. ChemistrySelect published by Wiley-VCH GmbH

the oxidation of benzyl alcohol depends strongly on the intensity of the light because a higher light intensity can provide more energy for the reaction. We suppose an enhanced interaction between CTF-PhTh and the absorbed reactants, and thus a promoted superoxide radical generation, eventually increasing the selectivity and conversion of benzyl alcohol.[54]

In addition, experiments at wavelengths of 450 nm and 365 nm were carried out under otherwise identical conditions (in Figure S6). Potentially due to the lower light intensity for 450 nm visible light (0.015 W cm^{-2}) compared to UV light, it took 10 hours to reach 31% conversion for CTF-PhTh, while the selectivity of benzaldehyde reached 100% and no further products were observed. Interestingly, at a wavelength of 500 nm (0.02 W cm^{-2}) no substrate conversion could be reached for phenyl-based CTFs, while only a minor conversion was obtained for thiophene-based CTFs, CTF-Th (4.6%), CTF-PhTh (1.8%), probably owing to the light absorbance threshold and the lower light energy. We also compared the catalytic performance of CTF-PhTh to that of the state-of-art catalysts (see Table S5). The conversion (44.9%), selectivity (100%), and TOF (0.449 mmol g^{-1}_{cat} h^{-1}) are in line with those of state-of-art catalysts. Noticeably, we used a light source with a very low input power of 0.8 W which is much lower than 250–500 W of the typical light source used in literatures again indicating the superior performance and high energy efficiency of the sulfur-containing CTFs in the photo-oxidation of benzyl alcohol.

To make a comparison with the reported CTF-Th@SBA-15 for photo-oxidation of benzyl alcohol and our catalytic system, CTF-Th@SBA-15 was synthesized according to Huang's work with slight modification.[28] This catalyst shows 91% conversion and full selectivity already after 1 hour (in Figure S7). Despite the superior catalytic activity of CTF-Th@SBA-15, the materials presented in this study enable a safe and facile synthesis under mild reaction conditions (no super acid added). In addition, the catalysts studied herein already provide good catalytic activity without the need for additional support material to increase the specific surface area.

To evaluate the recycling stability, the CTFs were reused in photo-oxidation of benzyl alcohol and washed by ethanol between the runs. Figure 10 illustrates the results. Both thiophene-based and phenyl-based CTFs possessed an excellent catalytic activity for at least six cycles with only minor loss in activity.

Inspired by the good catalytic activity of CTFs in the photo-oxidation of benzyl alcohol, we proceeded to further apply CTFs for the photo-oxidation of several other aromatic alcohols. Indeed, for most aromatic alcohols efficient oxidation to the corresponding aldehydes could be reached accompanied by further oxidation to the acids (in Table 1). Except for 4-fluorobenzyl alcohol and 4-methoxybenzyl alcohol as substrates (entry 3 and 6), CTF-PhTh and CTF-BiPh facilitated close to full conversion and high selectivity for the different substituted benzyl alcohols in photo-oxidation. We assign this excellent performance partly to a larger specific surface area for CTF-BiPh and sulfur promotion for CTF-PhTh, respectively (computational structure shown in Figure S4). In addition, the

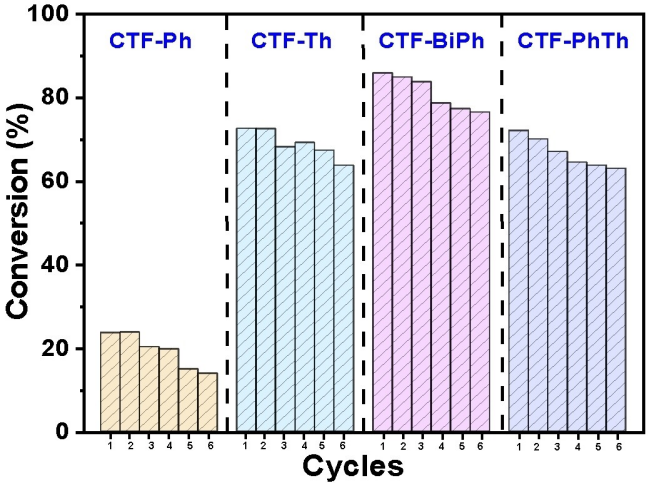

Figure 10. Recyclability of CTFs in the photo-oxidation of benzyl alcohol. Reaction conditions: benzyl alcohol (5 μmol), acetonitrile (5.0 mL), photocatalyst (5.0 mg), UV light ($\lambda = 365$ nm, 0.1 W cm^{-2}), 2 h, RT, O_2 balloon.

incorporated thiophene structural unit of CTF-Th could facilitate an efficient and selective transformation. CTF-Ph showed the lowest catalytic performance of the different CTF materials. However, it provided superior selectivity for the different substrates. Besides, the electronic effect caused by substituents on benzyl alcohol may be a reason affecting conversion. For example, 4-methyl benzyl alcohol holds an electron-donating group (–CH_3), while 4-fluorobenzyl alcohol holds an electron-withdrawing group (–F), respectively and both substrates only allow a low conversion compared to all the other heteroaromatic alcohols. Nevertheless, thiophene-based and phenyl-based CTFs enable the effective photo-oxidation of different substrates emphasizing their potential for a broader application in other photocatalytic reactions.[35]

2.2. Analysis of the probable photocatalytic mechanism

To better understand the reaction mechanism for the selective oxidation of benzyl alcohol over CTFs (CTF-PhTh as a representative), various radical scavengers were used in control experiments. As shown in Figure 11, no significant change in the reaction was observed by adding *tert*-butyl alcohol (TBA)[56–57] as a hydroxyl radical (·OH) scavenger in the oxidation of benzyl alcohol, indicating that hydroxyl radicals were not formed in the oxidation process and played a minor effect in the photocatalytic reaction. However, there was an abrupt decrease in conversion of 16% and 22% by the use of methanol as the photo-generated holes (h^+) scavenger and $AgNO_3$ as photo-generated electrons (e^-) scavenger[58] to suppress the photocatalytic oxidation of benzyl alcohol, indicating the photo-generated electrons and photo-generated holes are active parts in the catalytic process. The role of superoxide radical (O_2^-) and singlet oxygen ($^1O_2$) was confirmed by another control experiment under addition of p-benzoquinone (BQ)[59–60] and 9,10-diphenylanthracene (DPA)[61–62] as a

© 2020 The Authors. ChemistrySelect published by Wiley-VCH GmbH

Table 1. Scope of the photo-oxidation of aromatic alcohols over CTFs.

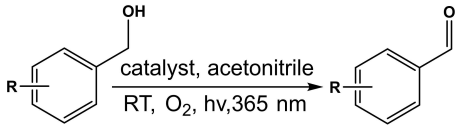

Entry	Substrate	Product	Catalysts	Conv.[a] [%]	Sel-1.[b]* [%]	Sel-2.[c]* [%]
1	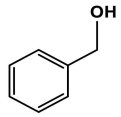 benzyl alcohol	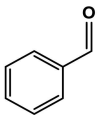	CTF-Ph	14.6	100	0
			CTF-Th	41.6	100	0
			CTF-BiPh	63.4	100	0
			CTF-PhTh	44.9	100	0
2	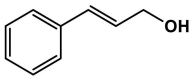 cinnamyl alcohol	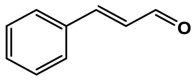 cinnamyl aldehyde	CTF-Ph	58.0	100	0
			CTF-Th	100	44.1	55.9
			CTF-BiPh	100	88.2	11.8
			CTF-PhTh	100	100	0
3	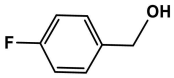 4-fluorobenzyl alcohol	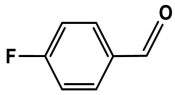 4-fluorobenzaldehyde	CTF-Ph	8.1	100	0
			CTF-Th	7.2	100	0
			CTF-BiPh	44.0	100	0
			CTF-PhTh	39.5	100	0
4	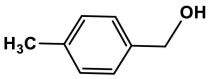 4-methyl benzyl alcohol	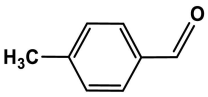 4-methyl benzaldehyde	CTF-Ph	24.9	100	0
			CTF-Th	56.8	100	0
			CTF-BiPh	100	81.4	18.9
			CTF-PhTh	97.8	85.1	14.9
5	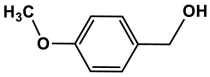 4-methoxybenzylalcohol	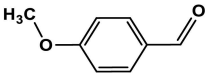 4-methoxy benzaldehyde	CTF-Ph	87.8	100	0
			CTF-Th	96.6	100	0
			CTF-BiPh	100	62.7	37.3
			CTF-PhTh	100	77.1	22.9
6	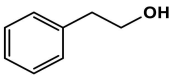 phenyl ethanol	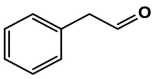 phenyl acetaldehyde	CTF-Ph	2.0	100	0
			CTF-Th	5.1	49.1	50.9
			CTF-BiPh	12.0	42.0	58.0
			CTF-PhTh	13.6	53.7	46.3

Reaction conditions: alcohol (5 μmol), acetonitrile (5.0 mL), photocatalyst (5.0 mg), UV light ($\lambda = 365$ nm, 0.1 W cm^{-2}), 1 h, RT, O_2 balloon. [a] Conv. is the conversion of aromatic alcohol, [b] Sel-1. is the selectivity of main product aldehyde, [c] Sel-2. is the selectivity of side-product corresponding acid. * Calculated solely based on the GC signals of these compounds assuming them to sum up to 100%.

superoxide radical and singlet oxygen scavengers. A reduced conversion of 7% and 26% was observed, showing that superoxide radical and singlet oxygen were formed in the photocatalytic reaction and acted as oxidant species in the catalytic cycle.

On the basis of the controlled experiments results in Figure 11, a possible photocatalytic oxidation mechanism of aromatic alcohols over CTFs was summarized in Scheme 2. Illuminating CTFs by UV or visible light leads to photo-generated carriers, and the excited electrons are driven to the conduction band, thus leaving holes in the valence band. Consequently, the photo-generated electrons/holes move to the surface of the CTFs, separately. Subsequently, molecular oxygen is reduced by photo-generated electrons to generate superoxide radical ($\cdot O_2^-$) or singlet oxygen ($^1O_2$), and the positively charged holes oxidize the alcohols adsorbed on the catalyst surface to generate carbocation. Eventually, the formed superoxide radicals or singlet oxygen further react with a

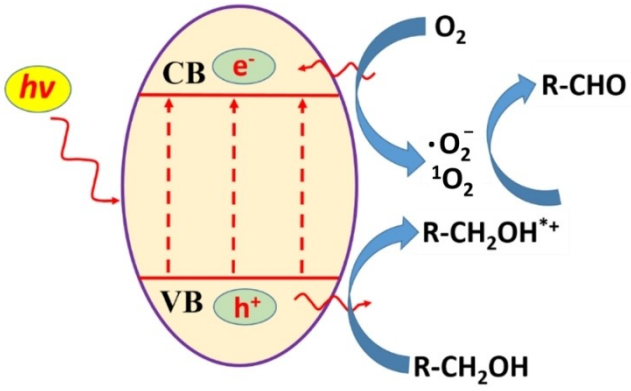

Scheme 2. The possible photocatalytic oxidation mechanism of aromatic alcohols over CTFs as photocatalysts.

© 2020 The Authors. ChemistrySelect published by Wiley-VCH GmbH

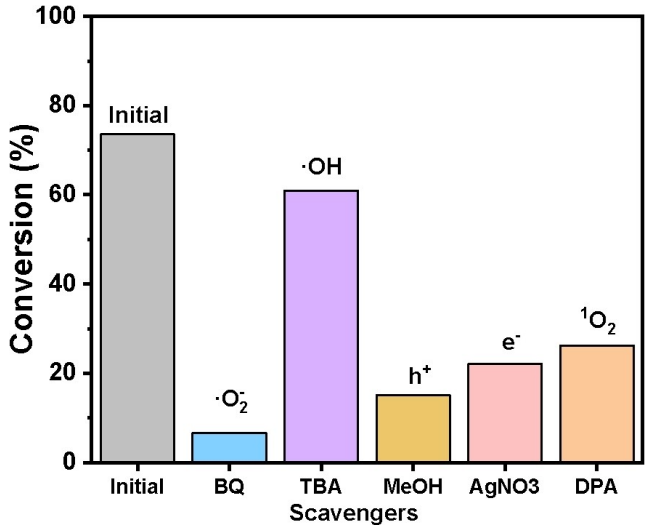

Figure 11. The controlled experiments for conversion of benzyl alcohol over CTF-PhTh in the presence of different radical scavengers. *Tert*-butyl alcohol (TBA) for hydroxyl radical (·OH) scavenger, methanol for the photo-generated holes (h^+) scavenger and $AgNO_3$ as photo-generated electrons (e^-) scavenger, *p*-benzoquinone (BQ) for superoxide radical (O_2^-) scavenger, and 9,10-diphenylanthracene (DPA) for singlet oxygen ($^1O_2$) scavenger. Reaction conditions: benzyl alcohol (5 μmol), acetonitrile (5.0 mL), photocatalyst (5.0 mg), 1 equiv. of scavenger, UV light ($\lambda = 365$ nm, 0.1 W cm^{-2}), 2 h, RT, O_2 balloon.

carbocation to produce the corresponding aromatic aldehydes.[63] The thiophene-based CTFs are due to their sulfur-content effective visible light-sensitive photocatalysts. Introducing a sp^3 orbital in the CTFs structure causes shrinkage of the valence band maximum (VBM) and the conduction band minimum promoting light absorption and improving charge separation/transfer. In line, narrower band gaps were obtained in CTF-Th and CTF-PhTh possessing superior photocatalytic performance.[47] Besides, the specific surface area appears also to be an important factor for the photocatalytic reaction, considering the activity of sulfur-free CTF-BiPh, which enables higher conversion and selectivity compared to CTF-Ph (surface area information in Table S3 and Figure S3, and experimental data in Figure 8).

3. Conclusions

In conclusion, thiophene-based covalent triazine frameworks could be synthesized via a polycondensation of amidines and aldehydes under mild reaction conditions. The materials showed promising performance in the photocatalytic oxidization of benzyl alcohol to the corresponding aldehyde irradiated by UV-visible light, with molecular oxygen as a mild oxidant. Superior catalytic performance was obtained most probably owing to the narrowed band gap of thiophene-based CTFs, since the incorporation of thiophene in covalent triazine framework allows effectively adjusting the intrinsic semiconductor properties, modifies the band gap structure and promotes the charge migration and separation. This work expands the available synthetic strategy to access tailored covalent organic frameworks possessing heteroatoms under mild conditions paving the way to metal-free polymer-based photocatalysts for the synthesis of fine chemicals.

Supporting Information Summary

Supplementary experimental section, supplementary figures, supplementary tables, and supplementary references.

Acknowledgements

Longfei Liao and Feng Zeng thank the China Scholarship Council for financial support. This work was supported by the Deutsche Forschungsgemeinschaft (DFG, German Research Foundation) under Germany's Excellence Strategy within the Exzellenzcluster 2186 "The Fuel Science Center" ID: 390919832. Jens Artz acknowledges a seed fund provided by RWTH Aachen University enabled by the German Research Foundation and the Excellence Initiative of the German Federal and State Governments. Open access funding enabled and organized by Projekt DEAL.

Conflict of Interest

The authors declare no conflict of interest.

Keywords: photo-oxidation · alcohols · catalyst · covalent triazine frameworks · thiophene

[1] Y. Chen, J. Zhang, M. Zhang, X. Wang, *Chem. Sci.* **2013**, *4* (8), 3244–3248.
[2] C. Parmeggiani, F. Cardona, *Green Chem.* **2012**, *14* (3), 547–564.
[3] T. Mallat, A. Baiker, *Chem. Rev.* **2004**, *104* (6), 3037–3058.
[4] Z. Guo, B. Liu, Q. Zhang, W. Deng, Y. Wang, Y. Yang, *Chem. Soc. Rev.* **2014**, *43* (10), 3480–3524.
[5] Y. Hu, G. Zhao, Q. Pan, H. Wang, Z. Shen, B. Peng, M. Muhler, *ChemCatChem.* **2019**, *11* (20), 5139–5144.
[6] M. Besson, P. Gallezot, *Catal. Today.* **2000**, *57* (1), 127–141.
[7] V. R. Choudhary, P. A. Chaudhari, V. S. Narkhede, *Catal. Commun.* **2003**, *4* (4), 171–175.
[8] F. Su, S. Mathew, G. Lipner, X. Fu, M. Antonietti, S. Blechert, X. Wang, *J. Am. Chem. Soc.* **2010**, *132* (46), 16299–301.
[9] M. J. Lima, P. B. Tavares, A. M. T. Silva, C. G. Silva, J. L. Faria, *Catal. Today.* **2017**, *287*, 70–77.
[10] X. Yang, X. Wang, J. Qiu, *Appl. Catal. A- Gen.* **2010**, *382* (1), 131–137.
[11] X. Yang, X. Wang, C. Liang, W. Su, C. Wang, Z. Feng, C. Li, J. Qiu, *Catal. Commun.* **2008**, *9* (13), 2278–2281.
[12] C. Yu, L. Fan, J. Yang, Y. Shan, J. Qiu, *Chem. Eur. J.* **2013**, *19* (48), 16192–16195.
[13] Y. Chen, J. Wang, W. Li, M. Ju, *Mater. Lett.* **2015**, *159*, 131–134.
[14] Y. Chen, W. Li, J. Wang, Q. Yang, Q. Hou, M. Ju, *RSC Adv.* **2016**, *6* (74), 70352–70363.
[15] C. Jiang, H. Wang, Y. Wang, H. Ji, *Appl. Catal. B.* **2020**, *277*, 119235.
[16] C. Xu, F. Yang, B. Deng, Y. Zhuang, D. Li, B. Liu, W. Yang, Y. Li, *J. Catal.* **2020**, *383*, 1–12.
[17] Q. Zhang, J. B. Liu, L. Chen, C. X. Xiao, P. Chen, S. Shen, J. K. Guo, C. T. Au, S. F. Yin, *Appl. Catal. B.* **2020**, *264*, 118529.
[18] L. Su, X. Ye, S. Meng, X. Fu, S. Chen, *Appl. Surf. Sci.* **2016**, *384*, 161–174.
[19] X. Wang, K. Maeda, A. Thomas, K. Takanabe, G. Xin, J. M. Carlsson, K. Domen, M. Antonietti, *Nat. Mater.* **2009**, *8* (1), 76–80.
[20] J. Liu, Y. Liu, N. Liu, Y. Han, X. Zhang, H. Huang, Y. Lifshitz, S. T. Lee, J. Zhong, Z. Kang, *Science.* **2015**, *347* (6225), 970–974.
[21] D. Masih, Y. Ma, S. Rohani, *Appl. Catal. B.* **2017**, *206*, 556–588.
[22] L. Zhou, H. Zhang, H. Sun, S. Liu, M. O. Tade, S. Wang, W. Jin, *Catal. Sci. Technol.* **2016**, *6* (19), 7002–7023.

© 2020 The Authors. ChemistrySelect published by Wiley-VCH GmbH

[23] J. Xu, L. Luo, G. Xiao, Z. Zhang, H. Lin, X. Wang, J. Long, *ACS Catal.* **2014**, *4* (9), 3302–3306.
[24] M. Liu, L. Guo, S. Jin, B. Tan, *J. Mater. Chem. A.* **2019**, *7* (10), 5153–5172.
[25] N. Tahir, C. Krishnaraj, K. Leus, P. Van Der Voort, *Polymer* **2019**, *11* (8), 1326.
[26] H. Wang, D. Jiang, D. Huang, G. Zeng, P. Xu, C. Lai, M. Chen, *J. Mater. Chem. A.* **2019**, *7* (40), 22848–22870.
[27] A. P. Cote, A. I. Benin, N. W. Ockwig, M. O'Keeffe, A. J. Matzger, O. M. Yaghi, *Science.* **2005**, *310* (5751), 1166–1170.
[28] X. Feng, X. Ding, D. Jiang, *Chem. Soc. Rev.* **2012**, *41* (18), 6010–6022.
[29] S. Y. Ding, W. Wang, *Chem. Soc. Rev.* **2013**, *42* (2), 548–568.
[30] C. Krishnaraj, H. Sekhar Jena, K. Leus, P. Van Der Voort, *Green Chem.* **2020**, *22* (4), 1038–1071.
[31] P. Kuhn, M. Antonietti, A. Thomas, *Angew. Chem. Int. Ed. Engl.* **2008**, *47* (18), 3450–3.
[32] S. Kuecken, J. Schmidt, L. Zhi, A. Thomas, *J. Mater. Chem. A.* **2015**, *3* (48), 24422–24427.
[33] S. Y. Yu, J. Mahmood, H. J. Noh, J. M. Seo, S. M. Jung, S. H. Shin, Y. K. Im, I. Y. Jeon, J. B. Baek, *Angew. Chem. Int. Ed. Engl.* **2018**, *57* (28), 8438–8442.
[34] Q. Jiang, L. Sun, J. Bi, S. Liang, L. Li, Y. Yu, L. Wu, *ChemSusChem.* **2018**, *11* (6), 1108–1113.
[35] L. Li, W. Fang, P. Zhang, J. Bi, Y. He, J. Wang, W. Su, *J. Mater. Chem. A.* **2016**, *4* (32), 12402–12406.
[36] S. Ren, M. J. Bojdys, R. Dawson, A. Laybourn, Y. Z. Khimyak, D. J. Adams, A. I. Cooper, *Adv. Mater.* **2012**, *24* (17), 2357–61.
[37] K. Wang, L. M. Yang, X. Wang, L. Guo, G. Cheng, C. Zhang, S. Jin, B. Tan, A. Cooper, *Angew. Chem. Int. Ed. Engl.* **2017**, *56* (45), 14149–14153.
[38] J. Artz, *ChemCatChem.* **2018**, *10* (8), 1753–1771.
[39] Y. Zhang, S. Jin, *Polymer.* **2019**, *11* (1), 31.
[40] M. Liu, K. Jiang, X. Ding, S. Wang, C. Zhang, J. Liu, Z. Zhan, G. Cheng, B. Li, H. Chen, S. Jin, B. Tan, *Adv. Mater.* **2019**, *31* (19), 1807865.
[41] M. Liu, Q. Huang, S. Wang, Z. Li, B. Li, S. Jin, B. Tan, *Angew. Chem. Int. Ed. Engl.* **2018**, *57* (37), 11968–72.
[42] E. G. Hohenstein, C. D. Sherrill, *J. Phys. Chem. A.* **2009**, *113* (5), 878–886.
[43] S. A. Gregory, A. K. Menon, S. Ye, D. S. Seferos, J. R. Reynolds, S. K. Yee, *Adv. Energy Mater.* **2018**, *8* (34), 1802419.
[44] K. Zhang, B. Tieke, *Macromolecules.* **2011**, *44* (12), 4596–4599.
[45] H. R. Zheng, J. S. Zhang, X. C. Wang, X. Z. Fu, *Acta Phys. -Chim. Sin.* **2012**, *28* (10), 2336–2342.
[46] X. Yang, X. Jiang, C. Zhao, R. Chen, P. Qin, L. Sun, *Tetrahedron Lett.* **2006**, *47* (28), 4961–4964.
[47] J. Zhang, M. Zhang, S. Lin, X. Fu, X. Wang, *J. Catal.* **2014**, *310*, 24–30.
[48] P. L. Wang, S. Y. Ding, Z. C. Zhang, Z. P. Wang, W. Wang, *J. Am. Chem. Soc.* **2019**, *141* (45), 18004–18008.
[49] W. Huang, B. C. Ma, H. Lu, R. Li, L. Wang, K. Landfester, K. A. I. Zhang, *ACS Catal.* **2017**, *7* (8), 5438–5442.
[50] D. Y. Osadchii, A. I. Olivos-Suarez, A. V. Bavykina, J. Gascon, *Langmuir.* **2017**, *33* (50), 14278–14285.
[51] T. Umebayashi, T. Yamaki, H. Itoh, K. Asai, *Appl. Phys. Lett.* **2002**, *81*(3), 454–456.
[52] D. Kong, X. Han, J. Xie, Q. Ruan, C. D. Windle, S. Gadipelli, K. Shen, Z. Bai, Z. Guo, J. Tang, *ACS Catal.* **2019**, *9* (9), 7697–7707.
[53] W. Huang, Z. J. Wang, B. C. Ma, S. Ghasimi, D. Gehrig, F. Laquai, K. Landfester, K. A. I. Zhang, *J. Mater. Chem. A.* **2016**, *4* (20), 7555–7559.
[54] J. Yu, J. Li, H. Wei, J. Zheng, H. Su, X. Wang, *J. Mol. Catal. A.* **2014**, *395*, 128–36.
[55] Y. Z. Chen, Z. U. Wang, H. Wang, J. Lu, S. H. Yu, H. L. Jiang, *J. Am. Chem. Soc.* **2017**, *139* (5), 2035–2044.
[56] Z. Kozmér, E. Arany, T. Alapi, G. Rózsa, K. Hernádi, A. Dombi, *J. Photochem. Photobiol. A.* **2016**, *314*, 125–32.
[57] P. K. Walia, M. Sharma, M. Kumar, V. Bhalla, *RSC Adv.* **2019**, *9* (62), 36198–203.
[58] X. Li, J. L. Shi, H. Hao, X. Lang, *Appl. Catal. B.* **2018**, *15*, 232, 260–7.
[59] M. Zhu, J. Lu, Y. Hu, Y. Liu, S. Hu, C. Zhu, *Environ. Sci. Pollut. Res. Int.* **2020**, 1.
[60] L. Zhang, D. Liu, J. Guan, X. Chen, X. Guo, F. Zhao, T. Hou, X. Mu, *Mater. Res. Bull.* **2014**, *59:*84–92.
[61] M. J. Steinbeck, A. U. Khan, M. Karnovsky, *J. Biol. Chem.* **1992**, *267*(19), 13425–33.
[62] S. Miyamoto, G. R. Martinez, M. H. Medeiros, P. Di Mascio, *J. Am. Chem. Soc.* **2003**, *125*(20), 6172–9.
[63] Y. Fang, X. Li, Y. Wang, C. Giordano, X. Wang, *Appl. Catal. B.* **2020**, *268*, 118398.

Submitted: October 27, 2020
Accepted: November 23, 2020

© 2020 The Authors. ChemistrySelect published by Wiley-VCH GmbH